Received: 3 October 2015 | Accepted: 21 November 2016

DOI 10.1002/hyp.11090

WILEY

RESEARCH ARTICLE

A conceptual hydrogeological model of ophiolitic aquifers (serpentinised peridotite): The test example of Mt. Prinzera (Northern Italy)

Stefano Segadelli[1] | Paolo Vescovi[1] | Kei Ogata[1] | Alessandro Chelli[1] | Andrea Zanini[2] | Tiziano Boschetti[1] | Emma Petrella[1] | Lorenzo Toscani[1] | Alessandro Gargini[3] | Fulvio Celico[1]

[1] Department of Physics and Earth Sciences "Macedonio Melloni", University of Parma, Parco Area delle Scienze, 157/A, Parma 43124, Italy

[2] Department of Civil, Environmental, Land Management Engineering and Architecture, University of Parma, Parco Area delle Scienze, 181/A, Parma, 43124, Italy

[3] Department of Biological, Geological, and Environmental Sciences, Alma Mater Studiorum University of Bologna, via Zamboni, 33, Bologna, 40126, Italy

Correspondence
Stefano Segadelli, Department of Physics and Earth Sciences "Macedonio Melloni" University of Parma, Parco Area delle Scienze, 157/A, 43124 Parma, Italy.
Email: stefanosegadelli@libero.it

Abstract

The main aim of this study is the experimental analysis of the hydrogeological behaviour of the Mt. Prinzera ultramafic massif in the northern Apennines, Italy. The analysed multidisciplinary database has been acquired through (a) geologic and structural survey; (b) geomorphologic survey; (c) hydrogeological monitoring; (d) physico-chemical analyses; and (e) isotopic analyses.

The ultramafic medium is made of several lithological units, tectonically overlapped. Between them, a low-permeability, discontinuous unit has been identified. This unit behaves as an aquitard and causes a perched groundwater to temporary flow within the upper medium, close to the surface. This perched groundwater flows out along several structurally controlled depressions, and then several high-altitude temporary springs can be observed during recharge, together with several perennial basal (i.e., low altitude) springs, caused by the compartmentalisation of the system because of high-angle tectonic discontinuities.

KEYWORDS

conceptual model, Italy, northern Apennine, perched groundwater, peridotite aquifer

1 | INTRODUCTION

The ophiolite bodies of the Alpine and Apennine belts are mostly composed of peridotites, serpentinites, gabbros, and basalts representing the original oceanic crust of the Ligure-Piemontese basin, developed in the Middle to Upper Jurassic, which separated the Europe plate from the Adria plate (Marroni et al., 2010). In the northern Apennines, these remnants of oceanic lithosphere are found within the Ligurian tectonic units and crop out in two palaeogeographic domains (Figure 1): the internal ligurides and external ligurides, which are identified on the basis of their current structural characteristics and their relationships with the associated sedimentary sequences (Abbate et al., 1986; Bortolotti et al., 2001; Elter, 1972; Elter, 1993).

The ophiolites are retained as one of the main aquifers within the northern Apennines (Gargini et al., 2014), but a few hydrogeological studies have been carried out worldwide to understand the behaviour of such aquifers (e.g., Boronina et al., 2003; Boronina et al., 2005; Dewandel et al., 2003; Dewandel et al., 2004; Dewandel et al., 2005; Join et al., 2005; Nikic et al., 2013). In this framework, an experimental study has been carried out in the test site of Mt. Prinzera ultramafic massif (Lat. 44°38′30″ N; Long. 10°5′ E; Figure 1) to define an effective and robust conceptual model, merging information from field-based geological, geomorphological, hydrogeological, hydrochemical, and isotopic analyses. This conceptual model has been then compared to those defined in other countries, in order to emphasise and discuss the main similarities and differences.

2 | MATERIAL AND METHODS

2.1 | Geological, structural, and geomorphological data

A detailed mapping survey was carried out in order to define and analyse those features that may control the hydrogeologic behaviour of the system, with emphasis on both the lithologic and the tectonic discontinuities. The fracture parameters inferred to influence groundwater flow (Singhal & Gupta, 1999; Bense et al., 2013) were quantitatively evaluated by collecting the following

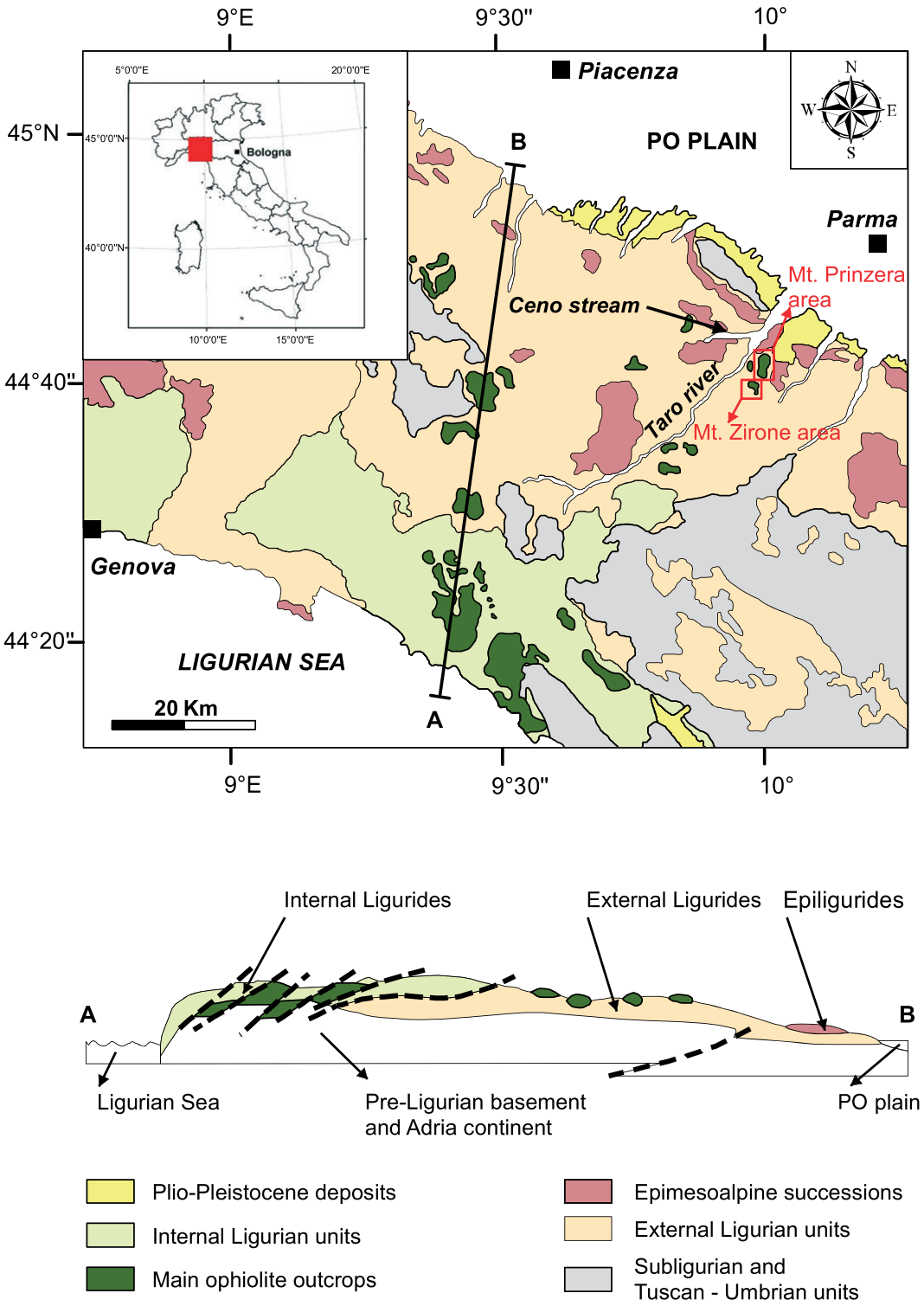

FIGURE 1 Tectonic sketch map and schematic geological section of the northern Apennines (modified from Marroni et al., 2010) and location of the study area (red box). Geographical coordinates in Gauss–Boaga. Latitude north and longitude east to Greenwich prime meridian reference

discrete structural data: (a) secondary fault-fracture frequencies, (b) number of fracture sets, (c) persistence, (d) aperture, and (e) spatial distribution. These fracture attributes were measured along a 73 m-long scan line intercepting at least three water-conductive tectonic lineaments. Such structures, identified in the geological mapping as major normal fault systems, host one of the monitored seasonal springs.

2.2 | Hydrogeological, hydrochemical, and isotopic data

The investigations were carried out from May 2012 to July 2013. Precipitation amounts and air temperature were measured through a meteorological station (Figure 2). The discharge of 13 springs (Figure 2) was monitored on a daily or weekly basis. Electrical conductivity (EC),

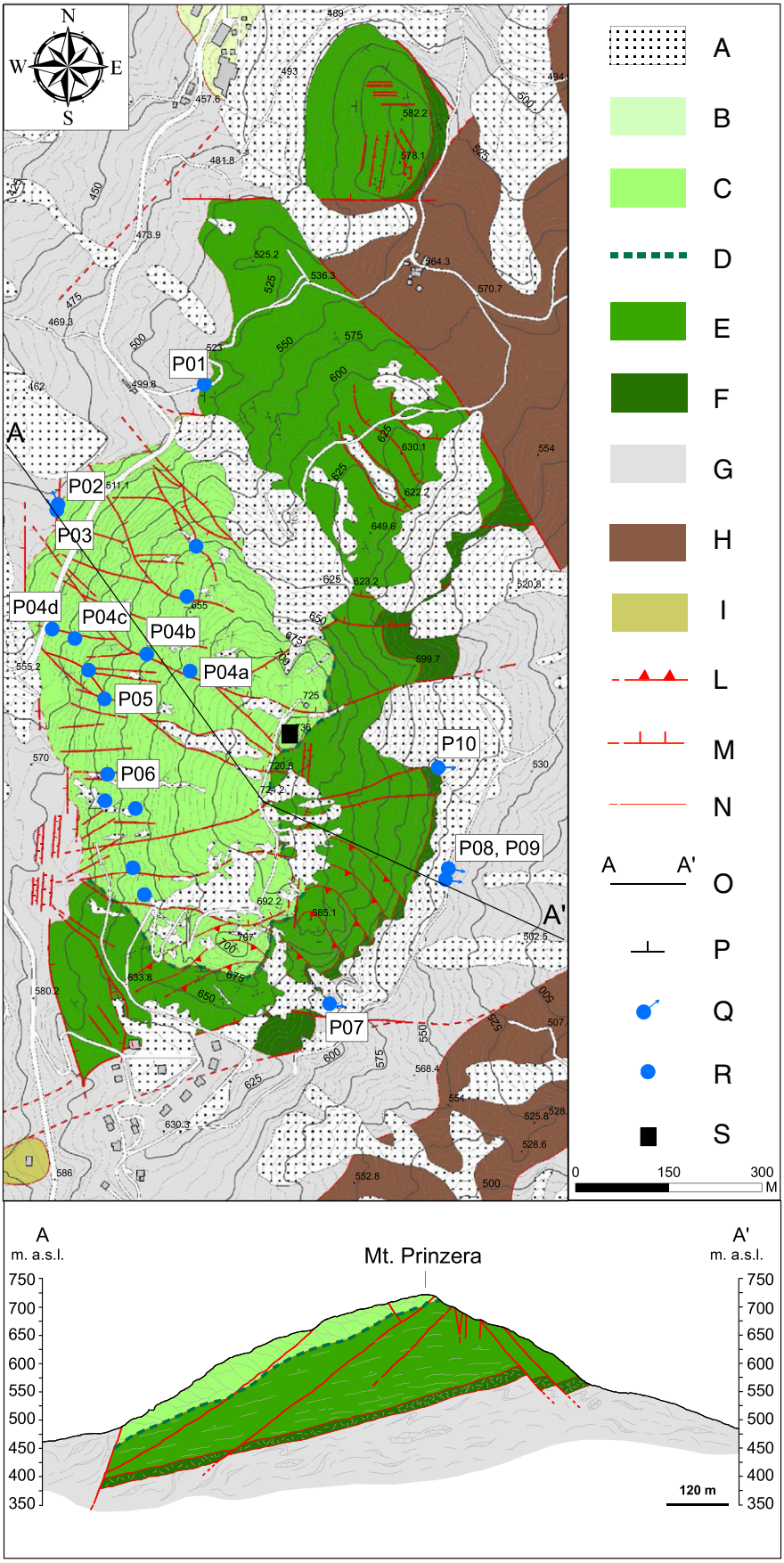

FIGURE 2 (a) Geological map of the study area. A, Quaternary deposits. B, Unit 5. C, Unit 4. D, Unit 3 (because of its short thickness, it is shown through the dashed line). E, Unit 2. F, Unit 1. G, Poligenic breccias in clay matrix. H, Helminthoid flysch. I, Peridotites. L, Thrust. M, Fault (the teeth indicates the downwards moved side). N, Tectonic contact. O, Geological cross section. P, Foliation attitude. Q, Perennial spring. R, Seasonal spring. S, Meteorological station. (b) Geologic cross section

temperature, and pH of spring waters were measured on the same basis, and chemical analyses (major and minor elements) were carried out twice, during the low-flow and the high-flow periods.

Stable isotope analyses ($\delta^{18}O$ and $\delta^{2}H$) were carried out on a monthly basis for both springwater and rainwaters. Local precipitations were collected at three stations located at different elevations. Stable isotope content was analysed on a daily or weekly basis, from January to March 2013, for four springs (P01, P02, P03, and P04b; Figure 2). Only $\delta^{18}O$ data have been shown hereafter.

Tritium content was analysed twice, during the low-flow and the high-flow periods, for five selected springs (P01, P02, P03, P04b, P07; Figure 2).

Labile parameters were determined in the field using a Polyplast BNC Hamilton glass electrode. EC at 25°C was measured using a Eutech Instrument (Cond 6+ model and pH 6+ model).

Physico-chemical analyses (major elements) were executed according to Boschetti et al., (2013). The stable isotopes were analysed at the Laboratorio di Geochimica Isotopica of the University of Parma (Italy) and the tritium content at the Laboratorio di Geochimica Isotopica of the University of Trieste (Italy). Isotopic ratios are reported in per mill relative to V-SMOW, and standard errors for $\delta^{2}H$ and $\delta^{18}O$ are ±1.0‰ and within ±0.1‰, respectively.

2.3 | Hydraulic data and hydrograph analysis

Because the Mt. Prizera is a natural reserve and the drillings are not allowed, two hydraulic tests, on a close area made up of the same ophiolitic sequence (Mt. Zirone area; Figure 1), have been performed and analysed. In particular, two tests with variable-rising heads were performed on existing monitoring wells with different characteristics (depth and screen length). In this kind of test, a pump allows to lower the head inside the monitoring well; once the pump is turned off, the rising of the head level is observed through an automatic probe. The estimation of the hydraulic conductivity is carried out through the following equation (Hvorslev, 1951):

$$k = \frac{A}{C(t_2 - t_1)} \ln\left(\frac{h_1}{h_2}\right)$$

where A is the internal cross section, h_1 and h_2 are the differences in total heads at times t_1 and t_2, respectively, and C is the shape factor that depends on the geometry of the injection zone (see for instance the works of Hvorslev, 1951; Cedergren, 1967; Chapuis, 1989).

The first interpretation of the base-flow analysis was carried out by Maillet (1905) and was based on the drainage of a simple reservoir. Maillet assumes that the discharge $Q(t)$ at time t of a spring is a function of the volume of water held in storage:

$$Q(t) = Q_0 e^{-\alpha t}$$

where Q_0 is the discharge at the start of the depletion cycle, t the time, and α the recession coefficient that represents both the storage and the hydraulic properties of the aquifer. This formulation considers the discharge proportional to the storage as $Q = 1/\alpha \times V$, where V is the storage capacity. Some hydrograph analyses (such as Wittenberg, 1999) keep into account nonlinearity between discharge and storage using nonlinear formulations such as power law functions.

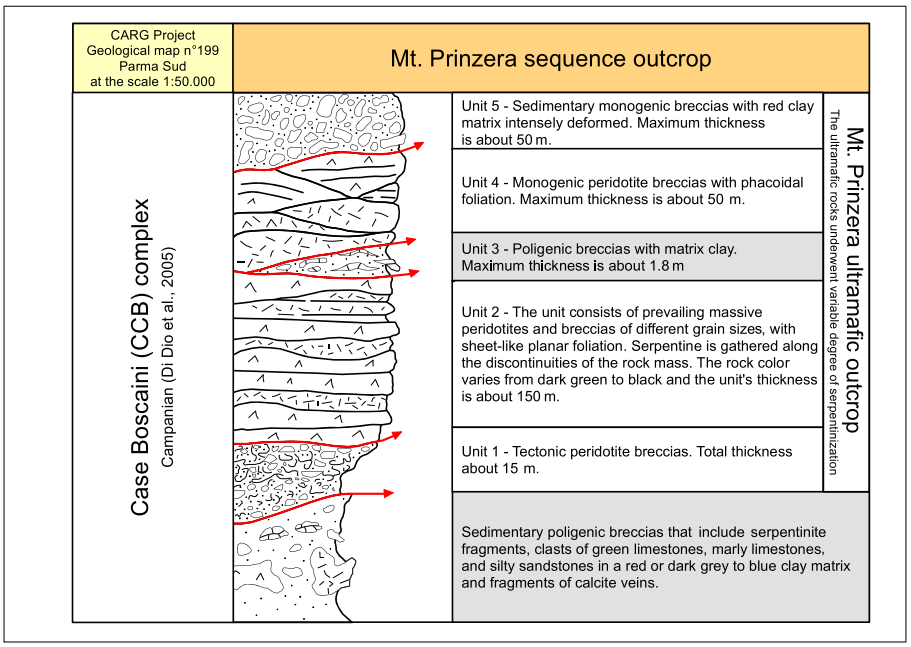

FIGURE 3 Schematic representation of the five units identified in the ultramafic medium and basal sedimentary polygenic breccias. The red line separates lithologic units with homogeneous characteristics

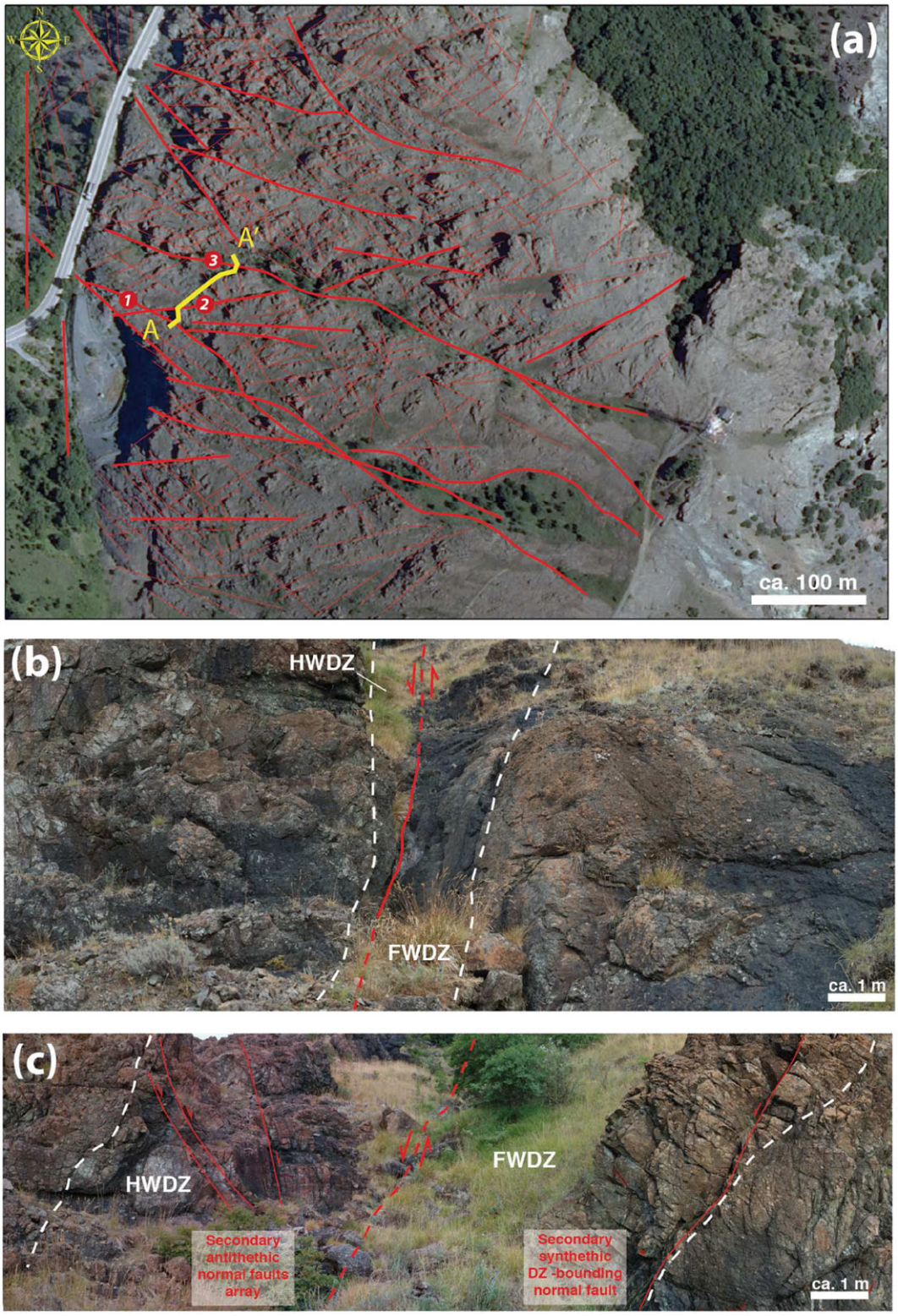

FIGURE 4 (a) Overview of the structural lineaments observed on the western slope of the massif with location (yellow line) of the measured scan-line (Figure 5). The main normal faults are labeled with thicker red lines. (b) Detail of the normal fault labeled as "1" in Figure 5 with labelling of the footwall (FWDZ) and hangingwall (HWDZ) damage zones. (c) Detail of the normal fault labeled as "3" in Figure 5 with the main structural elements highlighted (same as b). The analysed spring P04 is located within this fault zone (Figure 5)

The separation of the hydrograph was performed in order to estimate the contribution of the base-flow and of the quick-flow for each spring. The separation of the hydrographs has been carried out using several recursive digital filters (Lyne & Hollick, 1979; Chapman, 1991; USDA-ARS, 1999; Eckhardt, 2005), which were designed for stream-flow analysis. We noticed that the filter presented by Chapman (1991) is the one that better describes problems of nonperennial springs, and the filter proposed by Eckhardt (2005) is the one that better deals with perennial springs.

3 | RESULTS

3.1 | Geological, structural, geomorphological, and hydrogeological outcome

The main results are summarised as follows:

1) The Mt. Prinzera consists mainly of strongly layered serpentinised ultramafites extensively fractured at the meso-scale (Chelli et al., 2015; Figure 2). Because of structural-compositional heterogeneity on the vertical sequence, the entire body has been subdivided into five lithological units (campanian age, Di Dio et al., 2005), tectonically overlapped and gently tilted to the northwest (Figure 3). Between them, a low-permeability, discontinuous unit has been identified in a wide portion of the system. This unit behaves as an aquitard (unit 3);
2) At least four main deformation phases were recognised, the last one showing a clear extensional kinematic with high-angle faults (dips of the fault planes 50°–70°). These last high-angle tectonic

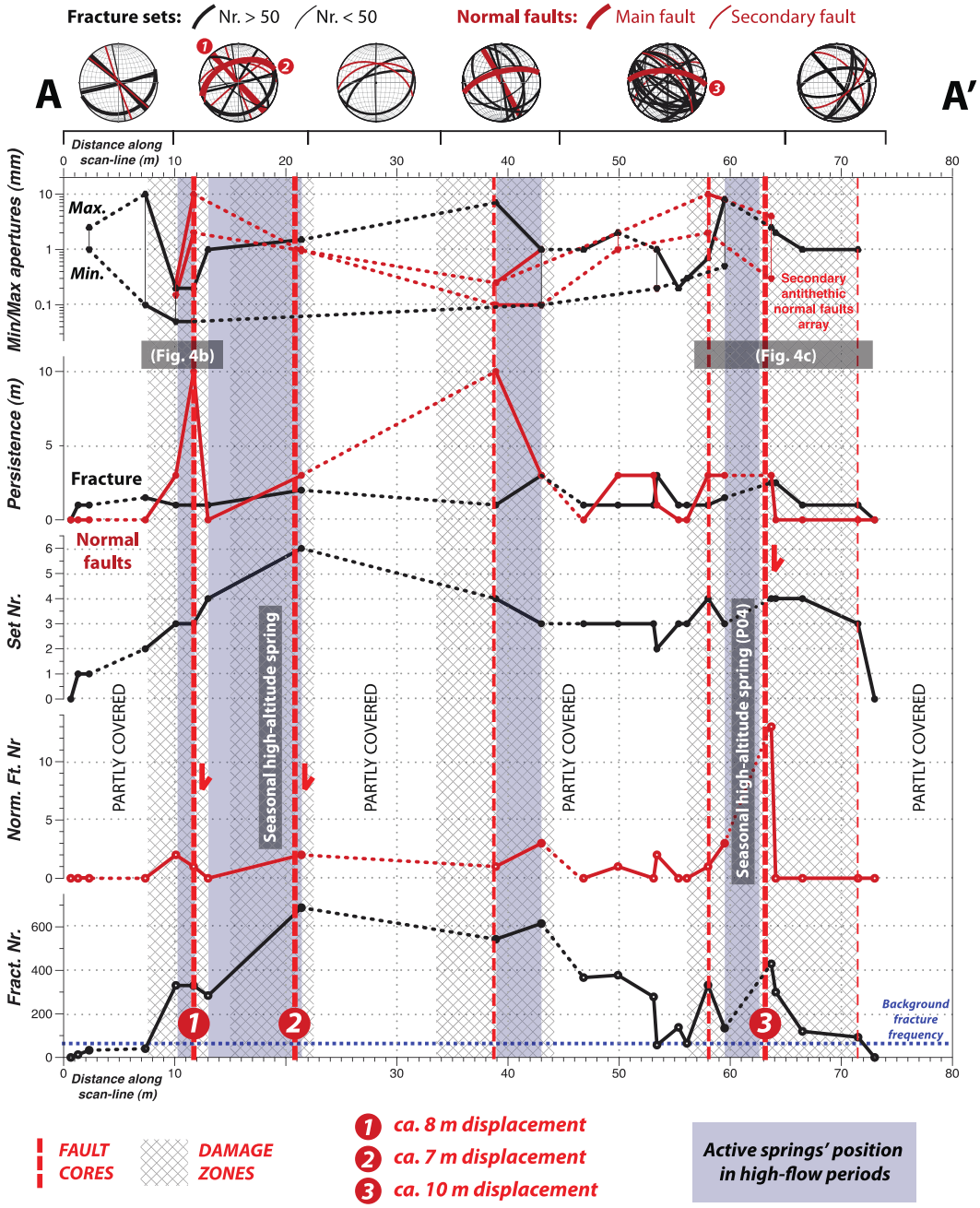

FIGURE 5 Diagram showing the lateral variation of the investigated fault-fracture structural parameters (e.g., fractures' and faults' count per meter, number of fractures' and faults' sets, persistence, and min and max apertures) along incremental steps of the measured scan line (location shown in Figure 4a; dotted lines link data gaps). The position of the encountered faults, the estimated extent of their damage zones, and the location of high-altitude springs is marked. In the top section, the spatial arrangement of the faults and fracture sets is illustrated in stereonets (equal angle, lower hemisphere; see explanation in the figure), showing the general structural attitude for consecutive segments of the measured scan line. Location of pictures shown in Figure 4b and c (and the position of analysed spring P04) is also indicated

discontinuities cut across the entire ultramafic sequence with listric-like shapes, and appear to be located along preceding tectonic lineaments trending roughly WNW-ESE;

3) Among these later normal faults, the ones characterised by greater offset can reach and displace the underlying impermeable unit, compartmentalising the deeper aquifer (see below). These normal faults show a maximum displacement around 10 m and lateral extents reaching the entire width of the ophiolite body (hundreds of meters), with scooped-curved shapes. In terms of fault architectural elements (e.g., Caine et al., 1996 and references therein), they are characterised by absent or discontinuous

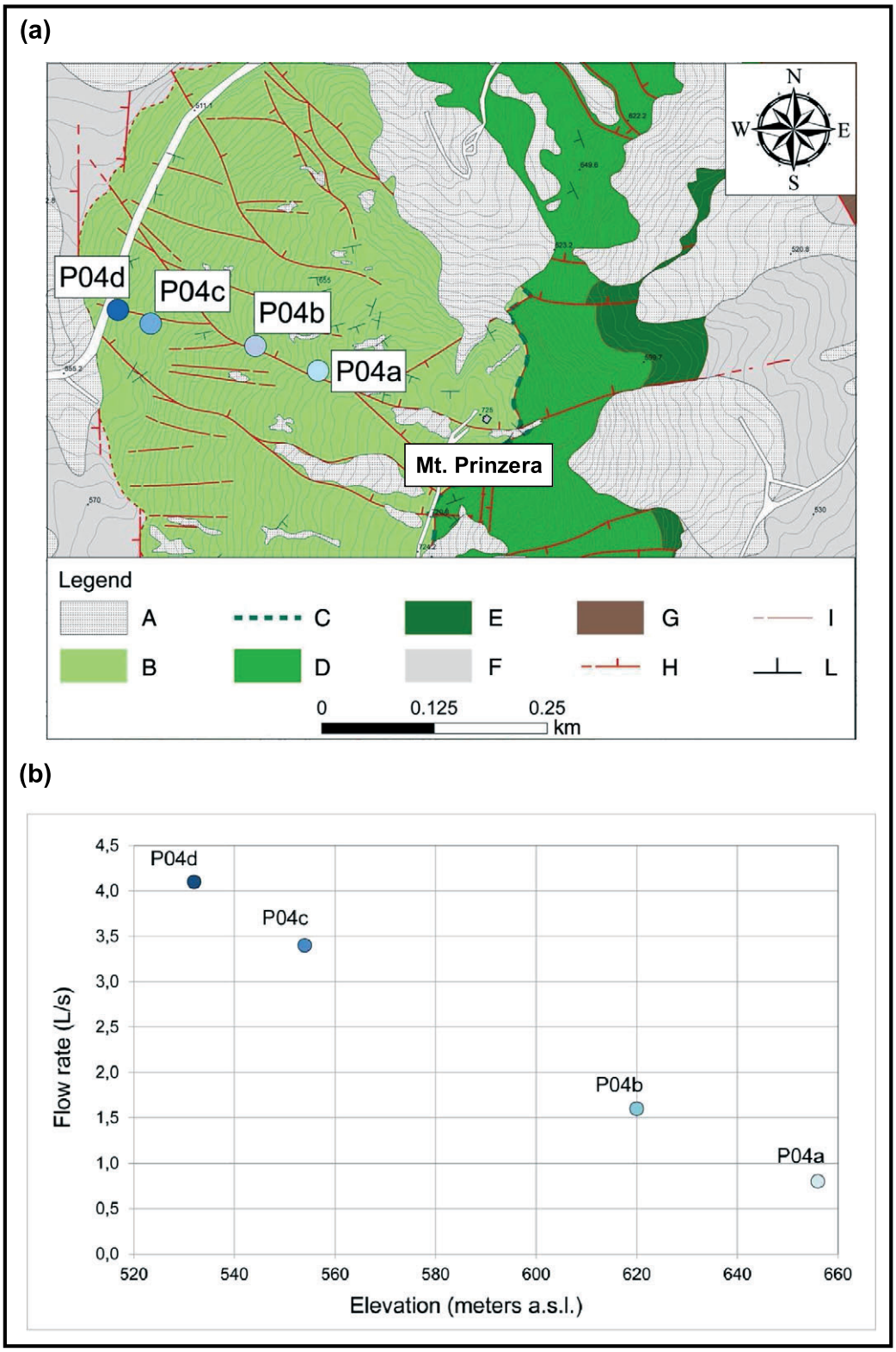

FIGURE 6 (a) location of seasonal spring P04 (A, quaternary deposits; B, unit 4; C, unit 3 [because of its short thickness, it is shown through the dashed line]; D, unit 2; E, unit 1; F, poligenic breccias in clay matrix; G, helminthoid flysch; H, fault (the teeth indicate the downwards moved side); I, tectonic contact; L, foliation attitude). (b) Seasonal spring discharge observed along the gully from the upper to the lower part of the incision

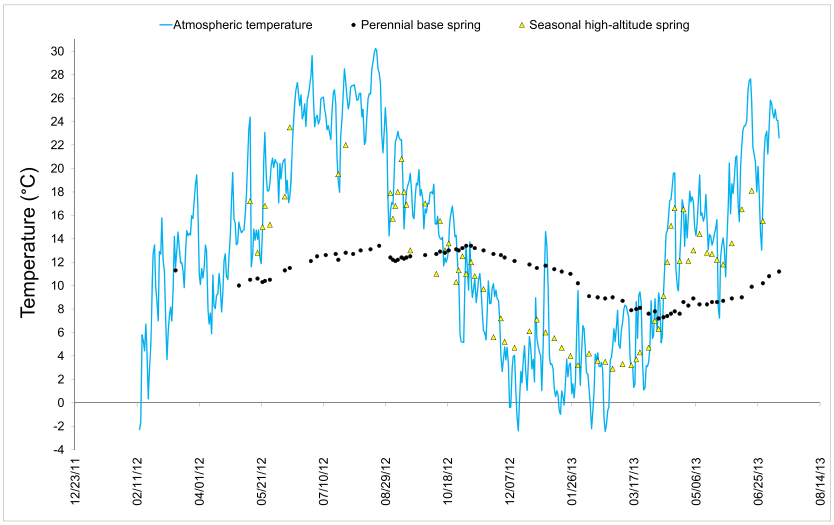

FIGURE 7 Thermal fluctuations in the atmosphere (blue line), at the perennial spring P03 (black dots), and at the high-altitude spring P04 (yellow triangle; dates are given in month/day/year)

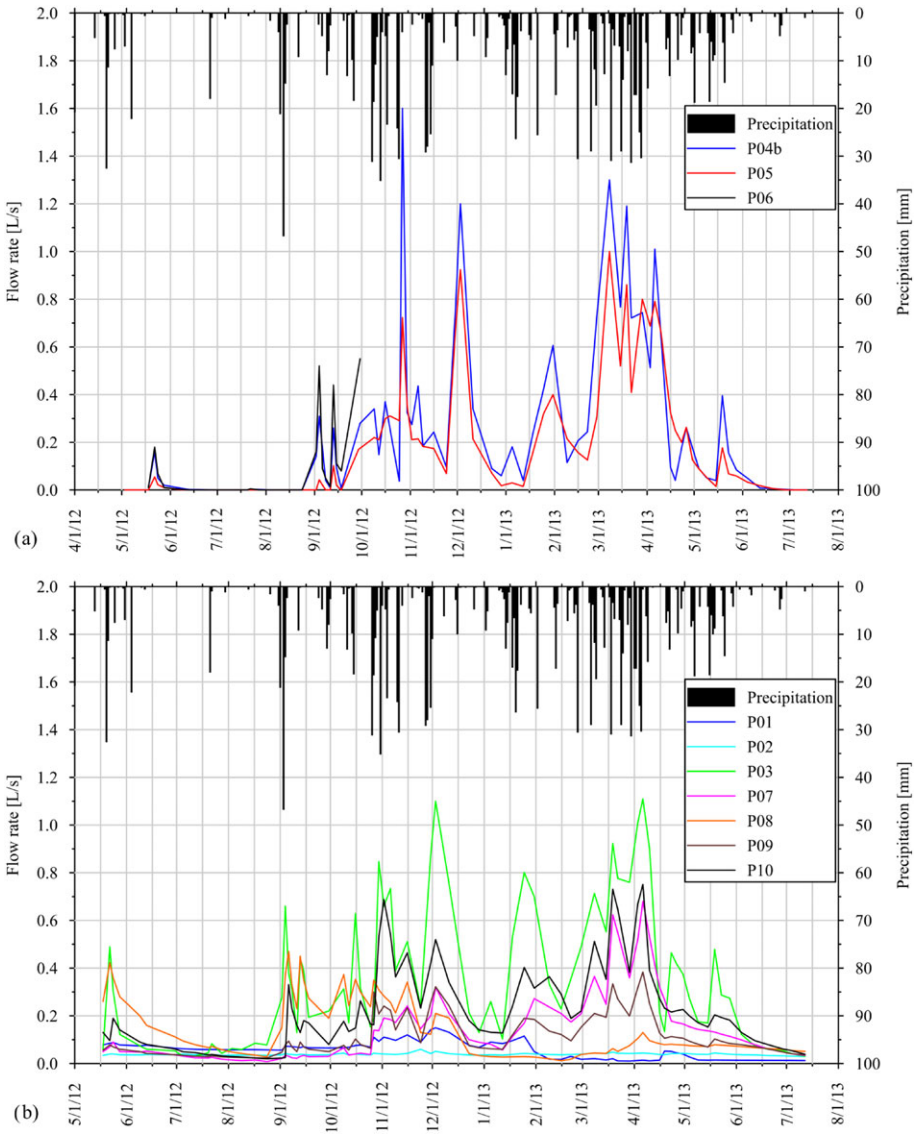

FIGURE 8 Springs hydrographs of (a) high-altitude seasonal springs and (b) perennial basal springs (dates are given in month/day/year)

millimeter- to centimeter-thick core zones consisting of one or more principal slip surfaces with pure to oblique dip-slip striations and lengths usually beyond the outcrop frame (up to ten meters). These narrow core zones are flanked on both sides by damage zones with variable extent (up to 15 m), comprising highly fractured lithologies locally crossed by secondary synthetic and antithetic shear planes width displacements less than 1 m, and one or more fracture (mostly joints) sets (see Figure 4). As summarised in Figure 5, a structural control appears to drive the preferential emergence of groundwater flow, supporting a scenario dominated by preferential along-fault permeability pathways. Direct relationships have been observed in matching the localisation of high-altitude springs to the combined increments of standard structural parameters (e.g., Singhal & Gupta, 2010), such as fracture secondary faults frequency (Nr./m), their persistency (i.e., length), the total number of sets, and spatial orientations (i.e., potential intersections). Less clear relationships are observed for the apparent fracture apertures. In particular, peaks in the linear fracture frequency (up to ca. 700 fractures per meter) above the background threshold (ca. 50–70 fractures per meter), along with the localised increase of differently oriented, interacting fracture sets are nicely correlated with the position of the most active high-altitude seasonal springs (such as for example P04 in Figure 5). In general, the main contribution to this along-fault enhanced permeability is mainly due to the mutually intercepting fracture sets of the different faults' damage zones.

The interplay of these structural attributes enhances localised fracture permeability in proximity of major normal faults (displacement > 5 m), being particularly efficient where their damage and process zones interact (see the example of the scan-line interval 56–71 m in Figure 5). Seasonal high-altitude springs are preferentially located in the (inner) damage zones of major normal faults, where the bulk of interconnected open fractures more likely occur. In this framework, the different fault zone architectural elements show different hydrological behaviours, as also observed in ancient, exhumed hydrocarbon or carbon dioxide reservoir-cap rock systems (e.g., Ogata et al., 2014).

Such fault rocks are often represented by an unconsolidated and loose breccia at the outcrop surface, locally altered into discontinuous soil profiles draping narrow-vegetated gullies with roughly rectilinear trends in map view;

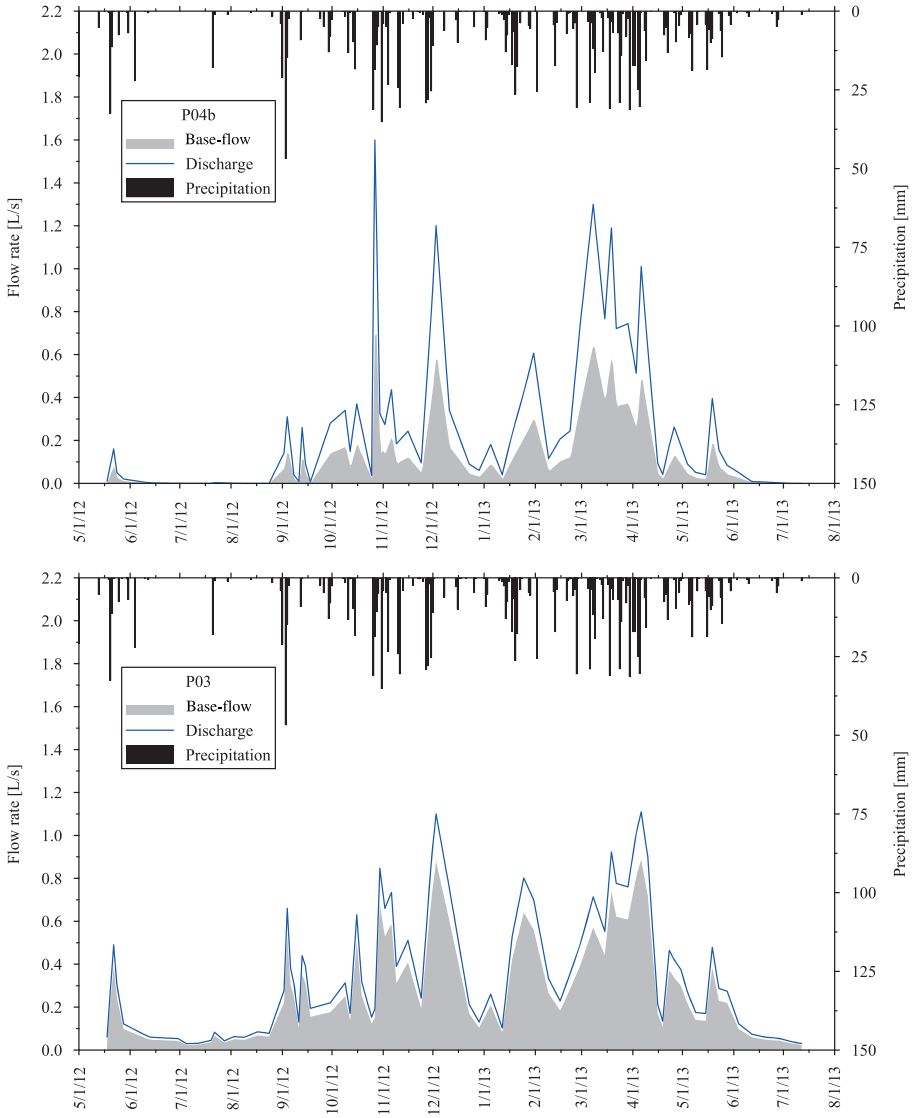

FIGURE 9 Observed discharge and baseflow related to the high-altitude spring P04 and the basal spring P03 versus daily precipitation (dates are given in month/day/year)

4) The ultramafites of Mt. Prinzera are bordered and underlain by low-permeability deposits that are predominantly characterised by polygenic breccias with fine-grained matrix. Therefore, from the hydrogeological point of view, the Mt. Prinzera is a well-delimited hydrostructure.
5) The ophiolitic rocks were investigated through several hydraulic tests that show an hydraulic conductivity ranging from 1.1 to 5.7 • 10^{-7} m/s, in agreement with the values (in the order of 10^{-7} m/s) obtained by Dewandel et al. (2005) in the Oman ophiolite aquifer.

3.2 | Time series analysis

Seven perennial and 10 seasonal springs have been identified (see Figure 2), respectively located along the contact between the ophiolitic medium and the low-permeability country rocks and within the serpentinised peridotites. However, the seasonal springs can be found only within the western part of the hydrostructure, where the lower permeability unit 3 causes enhanced vertical heterogeneity. Such springs flow out diffusely, along morphologic incisions, with progressive increasing in discharge observed from the upper to the lower part of the stream. This scenario has been analysed in detail along the spring P04, where this phenomenon is best represented (Figure 6).

The two spring types (perennial and seasonal) are characterised by a very different thermal regimes (Figure 7). The perennial basal springs show slight fluctuations over time, with maximum and minimum values shifted (60 to 70 days) with respect to the atmosphere, suggesting a relatively deep groundwater flow within the seasonal heterothermic zone. Differently, the seasonal high-altitude springs are characterised by important and frequent fluctuations, strictly related to the atmosphere, suggesting shallower groundwater flow within the daily heterothermic zone.

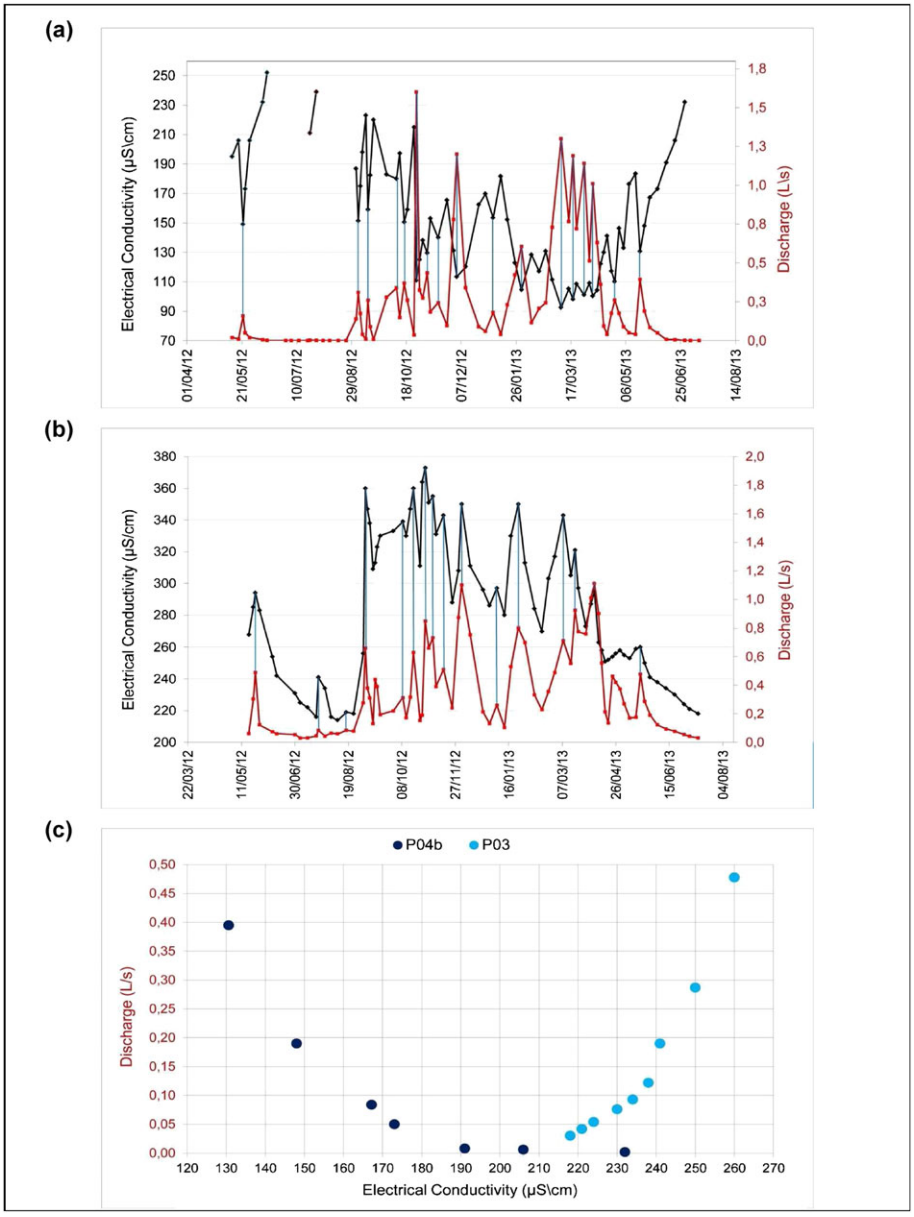

FIGURE 10 (a) Springs discharge versus electrical conductivity related to the perennial spring P03 and (b) the high-altitude spring P04b. (c) Test example (recession, undisturbed period) emphasising the direct relationship observed for perennial springs, and the inverse relationship observed for high-altitude springs (dates are given in month/day/year)

TABLE 1 Chemical data

Sample	Sampling data	T °C	Eh mV	pH At T° C	TDS mg/L	totN(−III) As NH4 mg/L	totS(−II) As HS mg/L	Cl mg/L	totS mg/L	totAlk As HCO3 mg/L	Ca mg/L	Mg mg/L	Na mg/L	K mg/L	Si mg/L	IB %
P01	28-may-2012	13.9	105	8.67	170	<0.04	<0.02	4.5	12	167	7.1	35.3	1.6	0.23	0.77	3.58
P02	28-may-2012	11.9	−34.1	11.08	114	0.17	0.83	20.8	5	68	8.7	0.2	29.8	0.40	0.85	−1.41
P03	28-may-2012	10.3	134	7.80	162	<0.04	<0.02	20.4	8	114	13.3	12.6	23.7	0.25	4.2	2.41
P04b	30-may-2012	14.6	67	7.76	128	<0.04	<0.02	3.6	3	126	4.0	23.6	1.6	0.17	8.4	−0.32
P05	28-may-2012	10.8	113	7.69	371	<0.04	<0.02	5.2	21	349	43.8	46.6	9.9	0.99	9.9	1.39
P06	28-may-2012	11.6	140	7.71	206	0.67	<0.02	4.7	17	167	13.4	32.1	1.4	0.17	7.2	2.36
P07	28-may-2012	13.0	129	8.32	309	0.66	<0.02	7.1	12	296	37.5	35.7	8.3	0.22	13.2	−1.26
P08	21-Nov-2011	12.5	565	8.15	237	---	<0.02	3.4	4	240	29.0	29.3	5.2	0.25	14.0	−0.28
P08	30-may-2012	12.5	222	7.95	262	<0.04	<0.02	4.1	5	267	31.3	30.3	5.6	0.14	15.6	−3.39
P09	30-may-2012	12.4	230	7.63	193	<0.04	<0.02	3.7	4	192	27.3	19.8	4.8	0.12	10.7	−2.04
P10	30-may-2012	11.7	105	7.89	211	<0.04	<0.02	4.2	15	182	21.1	28.8	3.5	0.13	6.5	2.42
P10	21-Nov-2011	11.7	90	8.14	188	---	<0.02	3.7	13	158	19.0	27.0	3.0	0.19	6.3	5.59

Note. --- = not analysed.

IB = ionic balance calculated by PHREEQCI, version 3.3 and *phreeqc.dat* thermodynamic database (Parkhurst & Appelo 2015).

Figures 8 and 9 show the hydrographs of both the perennial and seasonal springs. The comparison between the hydrographs and the rainfall distribution over time suggests the existence of (a) fast infiltration processes within the unsaturated zone and (b) possible short travel time from the ground to the spring. The Figure 8 allows also to estimate the delay between the precipitation and the peak of the flow hydrograph in about 1 to 2 days. Interesting information can be acquired merging the springs' hydrographs with the variations of EC over time (Figure 10a and b). In the perennial basal springs, EC increases with increasing discharge, whereas in the seasonal high-altitude ones EC decreases with increasing discharge. This suggests that (a) the perennial basal springs are fed by a deeper groundwater, with EC fluctuations dominated by variations of the hydraulic head over time (a rising head causes the mobilization of a huge volume of deeper and slower groundwater with higher salinity), and (b) the seasonal high-altitude springs are fed by shallow groundwater characterised by short residence time, with EC fluctuations dominated by fast mixing between fresh-infiltration water and pre-event groundwater during rainfalls causing significant recharge.

Considering the average recession coefficients, estimated from the Maillet equation, a really fast depletion (α in the order of 10^{-1} d^{-1}) was observed for the seasonal high-altitude springs (typical of higher permeability media and/or small basins), in contrast to the observations (α in the order of 10^{-2} d^{-1}) made for the base ones (typical of lower-permeability media and/or larger basins). The separation of the hydrographs was performed in order to estimate the contribution of (a) the base-flow (in the case study, the deeper and/or slower groundwater) and (b) the quick-flow (in the case study, the groundwater dominated by fresh-infiltration water) for each spring; Figure 9 shows an example of a high altitude (P04b) and a basal spring (P03). Table 2 shows the value of the estimated recession coefficients, the total discharged volume in the monitored period, and the contribution of the quick-flow and the base-flow for each spring. The P06 spring was monitored only for a short period that was not enough to allow a reliable hydrograph separation.

Considering the high-altitude spring (Figure 9 and Table 2) it is possible to see that the base-flow is about 50% of the total discharge. This confirms, as suggested by EC and temperature, the importance of fast infiltration processes and short travel time of fresh-infiltration waters from the ground to the high-altitude spring. While analyzing the basal

TABLE 2 Recession coefficient, total discharged volume observed in the period, quick- and base-flow

Spring	Recession coefficient α [1/d]	Discharged volume [Mm^3]	Quick-flow [Mm^3]	Base-flow [Mm^3]	Type
P01	0.005	2.05	1.64	0.41	Basal
P02	0.011	1.40	1.12	0.28	Basal
P03	0.117	11.80	9.43	2.37	Basal
P04b	0.344	8.50	4.25	4.25	High altitude
P05	0.335	6.42	3.21	3.21	High altitude
P07	0.041	4.93	3.94	0.99	Basal
P08	0.062	4.52	3.61	0.91	Basal
P09	0.046	3.92	3.13	0.79	Basal
P10	0.066	7.68	6.14	1.54	Basal

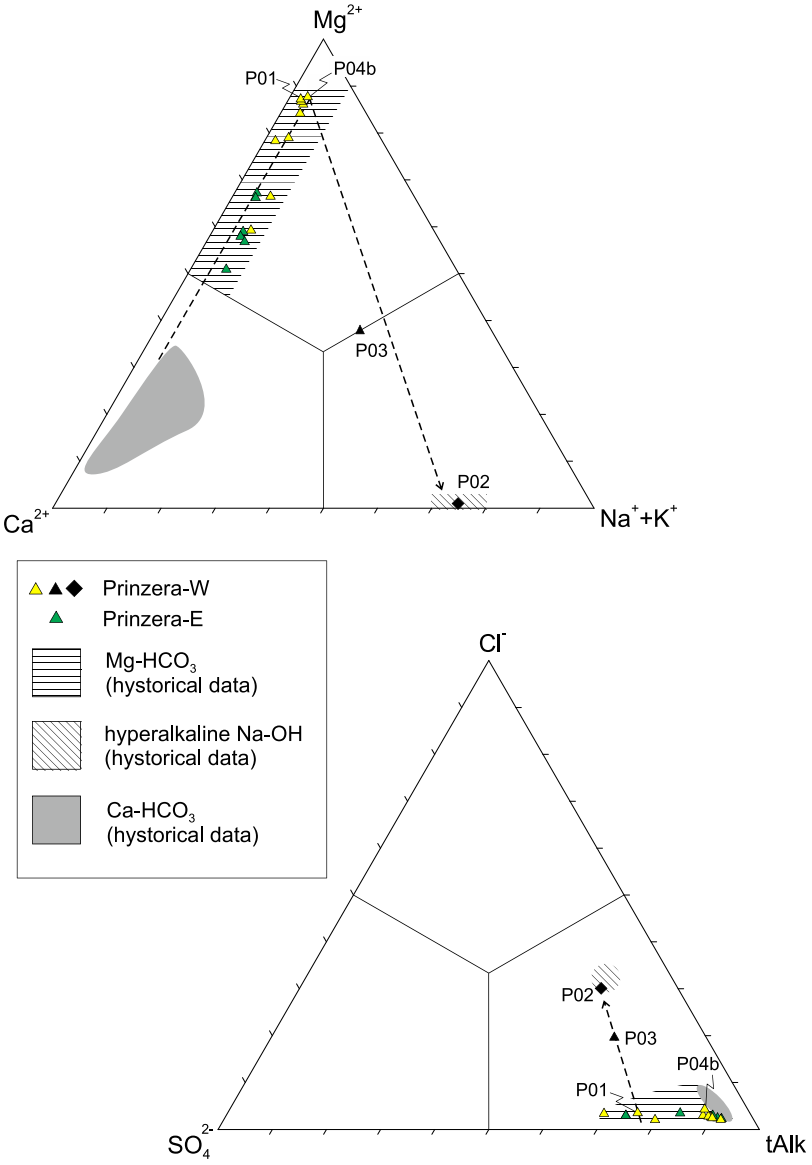

FIGURE 11 Ternary anions and cations classification diagrams of the sampled springs. Hystorical data areas include data from Venturelli et al. (1997), Boschetti and Toscani (2008), and Boschetti et al. (2013). Gray Ca-HCO_3 area represents local surface waters from Taro valley (Boschetti & Toscani, 2008)

spring, it is possible to notice that the base-flow is about 80% of the total discharge in the monitored period. This further confirms that perennial springs are fed mainly by deeper and/or slower groundwater.

3.3 | Water chemistry and isotopic analyses

Sampled springs show (Table 1) a main Mg-HCO_3 composition, fresh salinity (228 ± 64 mg/l), and an oxidizing redox potential (Eh = 160 ± 126 mV). Exceptions are represented by a hyperalkaline (pH > 10) Na-OH spring (P02), characterised by a lower salinity (114 mg/l) and redox potential (Eh = −34 mV), and a mixed spring (P01).

Figure 11 traced the possible evolution from a Ca-HCO_3, typical of surface water, to hyperalkaline passing through the Mg-HCO_3 composition. This chemical evolution from HCO_3^- to OH^- waters commonly occur in other peridotite aquifer worldwide (e.g., Barnes & O'Neil 1978; Cardace et al., 2015; Miller et al., 2016; Marques et al., 2008; Neal & Shand, 2002; Pawson, 2014; Stamatis & Gartzos, 1999), which

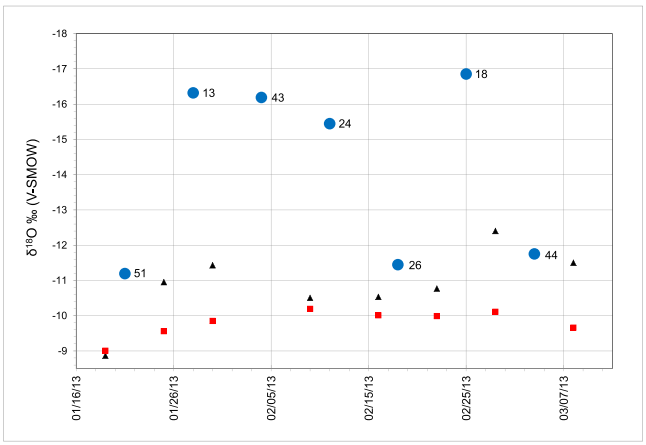

FIGURE 12 Temporal variations of $\delta^{18}O$ in perennial spring water (red square, P03) and in seasonal spring water (black triangle, P04b), and variations of weekly weighted mean $\delta^{18}O$ of rainwater (blue dots; numbers are the amount of rainfall in millimeters; dates are given in month/day/year)

was conventionally sorted by major ion chemistry into type I and type II waters, respectively (Neal & Stanger, 1984; 1985). Locally, it is the product of low-temperature reaction between meteoric water and ultramafic rocks, which is firstly accompanied by Mg-enrichment and then followed by Mg-decrease as consequence of the precipitation of Mg-bearing clay minerals (kaolinite, montmorillonite, saponite, and vermiculite) and serpentine, as supported by reaction-path modeling (Boschetti & Toscani, 2008; Boschetti et al., 2013). Furthermore, the decrease of carbonate in favor of hydroxide alkalinity (pH increase) and the lower redox in P02 (presence of reduced sulfur) are both evidences of an evolved composition in the water–rock interaction process and system closure at depth. Therefore, according to Boschetti and Toscani (2008), the evolutive path could be associated with the coexistence of two hydrologic circuits: shallow and fast (open to O_2-CO_2), where transition from Ca-HCO_3 to Mg-HCO_3 occurs quickly; and deep and slow (closed to O_2-CO_2), characterised by the switch from Mg-HCO_3 to Na-OH.

The data coming from the stable isotope investigations are here used to refine the details related to the interaction between fresh-infiltration waters and spring waters. In this framework, the stable isotope content of the perennial base springs P03 is characterised by slight fluctuations if compared to those detected in local rainwater (Figure 12), therefore showing a significant smoothing of the signal within both the unsaturated and saturated medium. This important but incomplete smoothing can be interpreted as the result of the mixing between groundwater bodies characterised by longer and

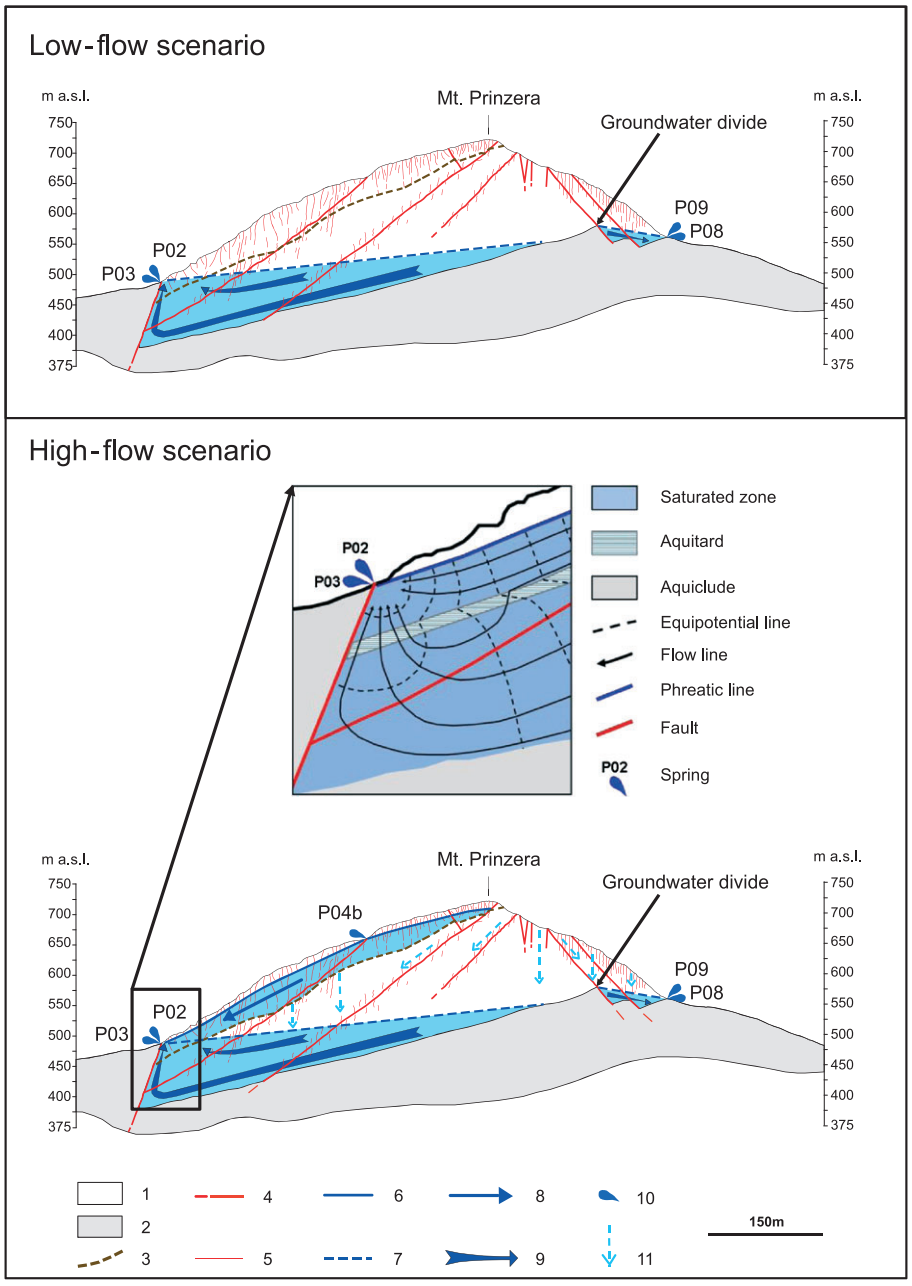

FIGURE 13 Hydrogeologic conceptual model of the Mt. Prinzera aquifer system. Legend 1, ultramafic aquifer; legend 2, aquiclude; legend 3, discontinuous aquitard; legend 4, fault; legend 5, fracture; legend 6, perched groundwater phreatic surface; legend 7, basal groundwater piezometric surface; legend 8, flow line of the perched groundwater; legend 9, flow line of the basal groundwater; legend 10, springs and their code; legend 11, infiltration within the unsaturated ultramafic medium

shorter residence times, with the longer ones dominating (in agreement with the results of the hydrograph separation analysis). Differently, the stable isotope content of seasonal high-altitude springs (P04b in Figure 12) is characterised by greater and more frequent fluctuations over time, strictly dependent from those observed in local rainwater. This observation strengthens the hypothesis of short travel time from the shallow underground to the seasonal springs and the dominance of fresh-infiltration water with respect to pre-event groundwater (in agreement with the results of the hydrograph separation analysis).

These interpretations are also in agreement with the tritium content. As matter of fact, the analysed seasonal high-altitude spring P04b is characterised by a content (8.1 TU) close to that observable in rainwaters, according to the hypothesised short-residence time of groundwater within this subsystem. The perennial base springs are characterised by a lower tritium content (5.4–7.0 TU), according to (a) the higher mean-residence time of groundwater within the deeper subsystem, and (b) the hypothesised mixing between deeper and shallower groundwater feeding these springs. The existence of deeper and longer groundwater pathways are definitively confirmed by the tritium content (91.0 TU) of the perennial hyper-alkaline spring (P02).

4 | CONCLUSIONS

The ophiolitic hydrostructure is characterised by layered and discontinuous heterogeneity (sensu, Freeze & Cherry, 1979), significantly influencing the hydrogeological behaviour of the system, which is due to the superimposition of different lithological units, mostly tectonically overlapped, characterised by different hydraulic properties. Seasonal high-altitude springs flow out diffusely along morphological incisions, showing that a perched and shallow seasonal groundwater migrates above the low-permeability unit 3.

Additional structural complexity is given by the occurrence of different set of faults, which play different roles from the hydrogeological point of view. First, the damage zones associated to the later, gravity-driven normal faults related to generalised unloading of the ophiolite mass during quaternary uplift-unroofing (and reworking former structural discontinuities achieved during the polyphased evolution of the Apennine orogen) created preferential along-fault fluid-flow pathways. In particular, the superficial groundwater leakage appears to be clustered where fault damage zones, process zones, and related fracture corridors mutually interact (see Figure 5).

These fault zones interrupt the lateral continuity of the low-permeability unit 3, emphasising the hydraulic interconnection between the perched and the basal aquifer (Figure 13). The lateral connectivity of the perched aquifer is not significantly influenced by these fault zones because of their vertical or lateral segmentation (with branches and relays) and the discontinuous, narrow-core zones likely affected by flaws causing diffused cross flow.

Furthermore, the main fault zones characterised by a significant displacement cross the underlying aquiclude, compartmentalising the deeper aquifer, and causing the basal and perennial groundwater to flow towards two sets of springs (on the western and eastern sides; Figure 13). This is further confirmed by the compositional attributes of the basal perennial springs flowing out along the western compartment, which are characterised by (a) methane of biotic origin, as supported by both isotopic (Boschetti et al., 2013) and biomolecular investigations (unpublished data); (b) high pH, up to 11; (c) negative redox potential; and (d) high chloride content (up to 21 mg/L). Conversely, the base perennial springs that flow out along the eastern boundary are characterised by (a) no methane, (b) pH always lower than 8.5, (c) positive redox potential, and (d) homogeneous chloride content (4.1 ± 1.4 mg/l).

Close to the western boundary, mixing between both the basal and the perched groundwater is achieved, creating a unique saturated zone. This scenario is characterised by a significant variation of the hydraulic head along with depth, with the shallower groundwater feeding the deeper one in the upgradient part, and vice versa close to the basal springs. Here, fluids related to deeper and prolonged pathways rise within the fault-related fracture network, locally causing a hyperalkaline spring to flow out.

When comparing this conceptual model with the few available in the scientific literature related to serpentinised peridotite, the following main suggestions can be made:

- the studied aquifer system is not characterised by a significant weathered horizon overlying the fissured bedrock; therefore, differently from Join et al. (2005), the hydrogeological behaviour of the whole system is not influenced by the coexistence of both a regolith-subsystem and a fracture-subsystem; however, according to the same authors, the shallower and the deeper groundwaters are interdependent despite the significant vertical heterogeneity of the aquifer system; moreover, in the case study, the shallower groundwater flows seasonally in a perched aquifer, due to the existence of an aquitard layer within the fractured peridotite, and an unsaturated zone is diffusely interposed between the shallower and the deeper groundwater;
- vertical heterogeneity was also found by Nikic et al. (2013), but also in this Serbian case, the contrast in permeability with depth is not due to the interposition of an aquitard layer within the fractured peridotite; the authors found that a role of utmost importance, from the hydraulic point of view, is played by the contrast in fracturing degree with depth; moreover, the authors observed a slow response of spring flow to atmospheric precipitation events, differently from observations made in the Prinzera aquifer system, where fast response and multiple-peak hydrographs have been detected; however, according to our studied system, Nikic et al. (2013) suggest the existence of higher permeability fault zones enhancing the hydraulic communication within the fractured medium;
- similarly, some differences can be found also comparing the Prinzera system with that analysed by Dewandel et al. (2005) in Oman; concerning the role of vertical heterogeneity, the hydrogeological functioning of the Oman ophiolite aquifer is not influenced by aquitard layers; in that case, the role of utmost importance is played by the contrast in permeability because of the superimposition of a fissured near-surface horizon (about 50 m thick) to a less fractured bedrock; however, also Dewandel

et al. (2005) suggest that deeper waters can rise relatively rapid along highly permeable and well-connected faults.

On the whole, an overall agreement can be found in the scientific literature concerning the existence of fault zones that act as conduit systems, enhancing fluid flow. Conversely, significant differences can be observed concerning the role of vertical heterogeneities on both the groundwater recharge and flow. As a matter of fact, different scenarios have been studied, where the vertical heterogeneity is linked to the coexistence of (a) a weathered horizon overlying a fissured bedrock, and/or (b) more fractured ophiolitic rocks overlying less fractured rocks, and/or (c) aquitard layers interposed within more permeable ophiolitic rocks (such as in the Prinzera aquifer system).

ACKNOWLEDGMENTS

We would like to thank Geostudi Srl (Parma) for supporting the field activities related to the hydraulic tests, and two anonymous reviewers for detailed and helpful reviews.

REFERENCES

Abbate, E., Bortolotti, V., Conti, M., Marcucci, M., Principi, G., Passerini, P., & Treves, B. (1986). Apennines and alps ophiolites and the evolution of the Western Tethys. *Memorie della Società Geologica Italiana*, *31*, 23–44.

Barnes, I., O'Neil, J. R., & Trescases, J. J. (1978). Present day serpentinization in New Caledonia, Oman and Yugoslavia. *Geochimica et Cosmochimica Acta*, *42*, 144–145.

Bense, V. F., Gleeson, T., Loveless, S. E., Bour, O., & Scibek, J. (2013). Fault zone hydrogeology. *Earth-Science Reviews*, *127*, 171–192.

Boronina, A., Renard, P., Balderer, W., & Christodoulides, A. (2003). Groundwater resources in the Kouris catchment (Cyprus): Data analysis and numerical modelling. *Journal of Hydrology*, *271*, 130–149.

Boronina, A., Balderer, W., Renard, P., & Stichler, W. (2005). Study of stable isotopes in the Kouris catchment (Cyprus) for the description of the regional groundwater flow. *Journal of Hydrology*, *308*, 214–226.

Bortolotti, V., Principi, G., & Treves, B. (2001). Ophiolites, Ligurides and the tectonic evolution from spreading to convergence of a Mesozoic Western Tethys segment. In G. B. Vai, & I. P. Martini (Eds.), *Anatomy of an orogen: The apennine and adjacent mediterranean basins*. (pp. 151–164). London: Kluwer Academic Publishers.

Boschetti, T., & Toscani, L. (2008). Springs and streams of the Taro-Ceno valleys (northern Apennine, Italy): Reaction path modeling of waters interacting with serpentinized ultramafic rocks. *Chemical Geology*, *257*, 76–91.

Boschetti, T., Etiope, G., Pennisi, M., Romain, M., & Toscani, L. (2013). Boron, lithium and methane isotope composition of hyperalkaline waters (northern Apennines, Italy): Terrestrial serpentinization or mixing with brine? *Applied Geochemistry*, *32*, 17–25.

Caine, J. S., Evans, J. P., & Forster, C. B. (1996). Fault zone architecture and permeability structure. *Geology*, *24*, 1025–1028.

Cardace, D., Meyer-Dombard, D. R., Woycheese, K. M., & Arcilla, C. A. (2015). Feasible metabolisms in high pH springs of the Philippines. *Frontiers in Microbiology*, *6*. doi:10.3389/fmicb.2015.00010

Cedergren, H. R. (1967). *Seepage, drainage, and flow nets*. New York: John Wiley and sons.

Chapuis, R. P. (1989). Shape-factors for permeability tests in boreholes and piezometers. *Ground Water*, *27*, 647–654.

Chelli, A., Segadelli, S., Vescovi, P., & Tellini, C. (2015). The geomorphological mapping as a tool in the groundwater study: The case of Mt. Prinzera rock aquifers (northern Apennines, Italy). *Journal of Maps*. doi:10.1080/17445647.2015.1072115

Chapman, T. G. (1991). Comment on "evaluation of automated techniques for baseflow and recession analyses" by R.J. Nathan and T.A. McMahon. *Water Resources Research*, *27*, 1783–1784.

Dewandel, B., Lachassagne, P., Bakalowicz, M., Weng, P., & Al, M. (2003). Evaluation of aquifer thickness by analyzing recession hydrographs. Application to the Oman ophiolite hard-rock aquifer. *Journal of Hydrology*, *274*, 248–269.

Dewandel, B., Lachassagne, P., & Qatan, A. (2004). Spatial measurements of stream baseflow, a relevant method for aquifer characterization and permeability evaluation. Application to a hard-rock aquifer, the Oman ophiolite. *Hydrological Processes*, *18*, 3391–3400.

Dewandel, B., Lachassagne, P., Boudier, F., Al-Hattali, S., Ladouche, B., Pinault, J. L., & Al-Suleimani, Z. (2005). A conceptual hydrogeological model of ophiolite hard-rock aquifers in Oman based on a multiscale and a multidisciplinary approach. *Hydrogeology Journal*, *13*, 708–726.

Di Dio, G., Martini, A., Lasagna, S., & Zanzucchi, G. (2005). *Note illustrative della Carta Geologica d'Italia alla scala 1:50.000, Foglio n°199 Parma Sud-Ovest*. S.EL.CA. Press .177pp

Eckhardt, K. (2005). How to construct recursive digital filters for baseflow separation. *Hydrological Processes*, *19*, 507–515.

Elter P. 1972. La zona ofiolitifera del Bracco nel quadro dell'Appennino Settentrionale. *Introduzione alla geologia delle Liguridi. 66° Congr. Soc. Geol. It., Guida alle escursione.* Pacini editore, Pisa, 35pp.

Elter, P. (1993). Detritismo ofiolitico e subduzione: Riflessioni sui rapporti Alpi-Appennino. *Memorie della Società Geologica Italiana*, *49*, 205–215 .Roma

Freeze, A., & Cherry, A. C. (1979). *Groundwater*. Upper Saddle River, USA: 604pp Prentice-Hall International Inc.

Gargini, A., De Nardo, M. T., Piccinini, L., Segadelli, S., & Vincenzi, V. (2014). Spring discharge and groundwater flow systems in sedimentary and ophiolitic hard rock aquifers: Experiences from northern Apennines (Italy). In J. M. Sharp (Ed.), I.A.H. Series n°20 *Fractured rock hydrogeology*. (pp. 129–146).

Hvorslev MJ. 1951. Time-lag and soil permeability in ground water observations. U.S. Army Engineering Waterways Experimental Station, Vicksburg, Miss., Bulletin 36.

Join, J. L., Robineau, B., Ambrosi, J. P., Costis, C., & Colin, F. (2005). Système hydrogéologique d'un massif minier ultrabisique de Nouvelle-Calédonie. *C.R. Geoscience*, *337*, 1500–1508.

Lyne VD, Hollick M. 1979. Stochastic time-variable rainfall-runoff modeling. In: Hydro. and Water Resour. Symp. Institution of Engineers Australia, Perth, Australia, pp. 89–92.

Maillet, E. (1905). *Essai d'hydraulique souterraine et fluviale*. Hermann, Paris: 218pp Librairie Scientifique. A.

Marques, J. M., Carreira, P. M., Carvalho, M. R., Matias, M. J., Goff, F. E., Basto, M. J., … Rocha, L. (2008). Origins of high pH mineral waters from ultramafic rocks, Central Portugal. *Applied Geochemistry*, *23*, 3278–3289.

Marroni, M., Meneghini, F., & Pandolfi, L. (2010). Anatomy of the Ligure-Piemontese subduction system: Evidence from late cretaceous-middle Eocene convergent margin deposits in the northern Apennines, Italy. *International Geology Review*, *52*, 1160–1192. doi:10.1080/00206810903545493

Miller, H. M., Matter, J. M., Kelemen, P., Ellison, E. T., Conrad, M. E., Fierer, N., … Templeton, A. S. (2016). Modern water/rock reactions in Oman hyperalkaline peridotite aquifers and implications for microbial habitability. *Geochimica et Cosmochimica Acta*, *179*, 217–241. doi:10.1016/j.gca.2016.01.033

Neal, C., & Shand, P. (2002). Spring and surface water quality of the Cyprus ophiolites. *Hydrology and Earth System Sciences*, *6*, 797–817.

Neal, C., & Stanger, G. (1984). Calcium and magnesium-hydroxide precipitation from alkaline groundwaters in Oman, and their significance to the process of serpentinization. *Mineralogical Magazine*, *48*, 237–241.

Neal, C., & Stanger, G. (1985). Past and present serpentinisation of ultramafic rocks; an example from the Semail Ophiolite Nappe of Northern

Oman. In J. I. Drever (Ed.), *The chemistry of weathering*) Springer, Nato Science Series. 10.1007/978-94-009-5333-8_15

Nikic, Z., Sreckovic-Batocanin, D., Burazer, M., Ristic, R., Papic, P., & Nikolic, V. (2013). A conceptual model of mildly alkaline water discharging from the Zlatibor ultramafic massif, western Serbia. *Hydrogeology Journal*, *21*, 1147–1163.

Ogata, K., Senger, K., Braathen, A., & Tveranger, J. (2014). Fracture corridors as seal bypass systems in siliciclastic reservoir cap rock successions: Field-based insights from the Jurassic Entrada formation (SE Utah, USA). *Journal of Structural Geology*, *66*, 162–187.

Parkhurst DL, Appelo CAJ. 2015. Description of input and examples for PHREEQC version 3- a computer program for speciation, batch-reaction, one-dimensional transport, and inverse geochemical calculations. http://wwwbrr.cr.usgs.gov/projects/GWC_coupled/phreeqc/phreeqc3-html/phreeqc3.htm

Pawson (2014). *Abiotic methane formation at the Dun Mountain ophiolite*. New Zealand: Master Degree Thesis, University of Canterbury, Christchurch, New Zealand.

Singhal, B. B. S., & Gupta, R. P. (1999). *Applied hydrogeology of fractured rocks*. Kluwer Academic Publishers .400pp

Singhal, B. B. S., & Gupta, R. P. (2010). *Applied hydrogeology of fractured rocks*. Hamburg London New York: Springer, 430pp.

Stamatis, G., & Gartos, E. (1999). The silica supersaturated waters of northern Evia and eastern Central Greece. *Hydrological Processes*, *13*, 2833–2845.

USDA-ARS (U.S. Department of Agriculture-Agricultural Research Service) 1999. Soil and water assessment tool, SWAT: Base flow filter program. Available at http://www.brc.tamus.edu/ swat/soft_base flow.html. Accessed in September 2005.

Venturelli, G., Contini, S., Bonazzi, A., & Mangia, A. (1997). Weathering of ultramafic rocks and element mobility at Mt. Prinzera, northern Apennines, Italy. *Mineralogical Magazine*, *61*, 765–778.

Wittenberg, H. (1999). Baseflow recession and recharge as nonlinear storage processes. *Hydrological Processes*, *13*, 715–726.

How to cite this article: Segadelli S, Vescovi P, Ogata K, Chelli A, Zanini A, Boschetti T, Petrella E, Toscani L, Gargini A, Celico F. A conceptual hydrogeological model of ophiolitic aquifers (serpentinised peridotite): The test example of Mt. Prinzera (Northern Italy). *Hydrological Processes*. 2016. doi: 10.1002/hyp.11090